Computational redesign of the test section for the Boeing/AFOSR Mach 6 Quiet Tunnel

H. Naiman and D. D. Knight
Rutgers – The State Universiy of New Jersey
98 Brett Road, Piscataway, NJ 08854, USA

Abstract

A proposed new design for the test section of the Boeing/AFOSR Mach 6 Quiet Tunnel is evaluated using CFD. The proposed design expands the diameter of the test section so that shock waves from the nose of the model impinge on a shear layer before reaching the wall boundary layer, as this configuration appears less likely to separate the upstream nozzle wall boundary layer. The purpose of this study is to predict what sorts of shocks and shear layers would result from such an expansion, and if they would penetrate into the test region. The unsteady, laminar, compressible Navier Stokes equations are solved for several cone sizes. Blunter cones are examined to determine how large a cone can fit in the test section before the tunnel unstarts, and it is found that for angles greater than 30° unstart occurs.

1. Introduction

One of the major challenges in hypersonic flow research is the accurate prediction of transition. The location and extent of laminar-turbulent transition is a critical parameter in hypersonic vehicle design. The transition location affects estimates of aerodynamic heating, skin friction drag and other boundary layer properties. Transition experiments have been carried out in conventional ground testing facilities for decades. However, most of the experimental data obtained from these facilities are contaminated by the high levels of noise that radiate from the turbulent boundary layers normally present on the nozzle walls. The effects of this acoustic noise are profound. These high noise levels can cause transition to occur an order of magnitude earlier than in flight[1]. Not only is the location of transition affected, but the parametric trends for transition can also be dramatically different from those in flight [2].

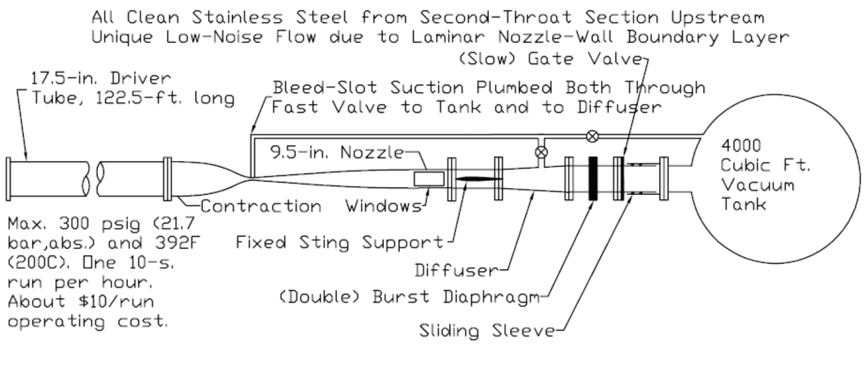

Figure 1: Schematic of the BAM6QT

Quiet flow wind tunnels have been developed to simulate hypersonic flow in flight, where the noise levels are very low. A quiet wind tunnel is characterized by laminar boundary layers in the test section. A review of the various efforts worldwide to develop quiet tunnels is provided in Ref. 3. A Mach-3.5 tunnel was the first to be successfully installed at NASA Langley in the early 80's. This was followed by a quiet Mach-6 hypersonic facility in the mid-90's. Unfortunately, this nozzle was removed from service due to a space conflict, and is now being reinstalled at Texas A&M. The Boeing/AFOSR Mach-6 Quiet Tunnel (BAM6QT) at Purdue University was constructed during 1995-2001. It is, at present, the only operational hypersonic quiet tunnel anywhere in the world[4].

The BAM6QT is designed as a Ludwieg tube (Figure 1). A Ludwieg tube is a long pipe with a converging-diverging nozzle on the end, from which flow exits into the nozzle, test section and second throat. A diaphragm is placed downstream of the test section. When the diaphragm bursts, an expansion wave travels upstream through the test section into the driver tube. Expansion wave reflections occur for a period of time during which the flow remains quiet. Figure 2 shows the nozzle. The region of useful quiet flow lies between the characteristics marking the onset of uniform flow, and the characteristics marking the upstream boundary of acoustic radiation from the onset of turbulence in the nozzle wall boundary layer.

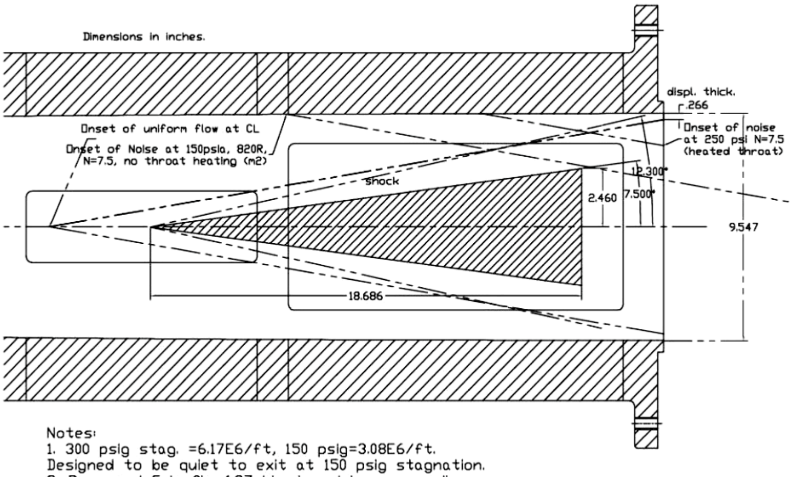

Figure 2: Quiet flow region in test section

Although slender vehicles are the primary concern in many transition experiments, blunt vehicles are also affected by transition[5]. Shocks emanating from the nose of the test cone and bow shocks from blunter models interact with the boundary layer on the tunnel wall. While disturbances in supersonic flow can only travel downstream, disturbances in the subsonic boundary layer flow in the test section can lead to separated flow upstream in the tunnel nozzle[6]. Laminar boundary layers are more likely to separate than turbulent ones, so shock/boundary layer interactions are more likely to affect upstream flow in a quiet tunnel, which has laminar boundary layers at high Reynolds numbers. Laminar shock/boundary-layer interactions are thus a critical issue for determining the largest possible model that can be started in the quiet tunnel.

1.2 Objective

Computations are performed for the test section of the BAM6QT to determine if expanding this section would allow larger blunt models to be tested. Separation of the upstream boundary layer is often induced when strong bow shocks from blunt models interact with the nozzle wall boundary layer[7]. The idea is to have the bow shock from a model impinge on a shear layer before reaching the wall boundary layer, as this may mitigate the upstream propagation of disturbances and the separation of the upstream boundary layer[8]. On the other hand, the the shear layer generated by expanding the section may grow and effectively reduce the useful test cross-section. The purpose of this analysis is to predict what sorts of shocks and shear layers would result from such an expansion, and if this new design would allow larger blunt models to be tested. Several cone sizes at zero angle of attack with a 5.5-inch base diameter are considered, with half-angles ranging from 15° to 75°, in order to determine how large a cone could fit in the test section before the tunnel unstarts.

2. Methodology

Six axisymmetric cases were run in total: one of the empty section, and five of the section with 15°, 20°, 30°, 50°, and 75° half-angle cones with a 5.5-inch base diameter. The empty section and the 15° half-angle cone had a 10° compression corner, but all other computations used a more gradual 1° compression (Figure 3). The grids were generated with GridPro[9]. The domain for the empty section consisted of one zone with 23,760 cells (100 x 241) and the domains for the cone cases consisted of four zones and contained approximately 39,000 points. Grid clustering was performed with a stretching parameter of 1.105 and a first cell height of 10^{-5} ft along the wall and cone surfaces in order to resolve the boundary layers (Figure 4).

2.1 Boundary conditions

The boundary conditions are listed in Table 1. The inflow boundary condition was a user-specified flow with a boundary layer thickness corresponding to a laminar boundary layer that had been developing since the stagnation point at the bleed lip near the tunnel throat, and a uniform Mach 6.15 freestream flow. The boundary layer profile contained 40 points and was calculated with EDDYBL[10], assuming a stagnation pressure and temperature of 90 psi and 433 K. The initial conditions were chosen such that the flow was accelerated from rest by an incoming shock wave. These conditions do not simulate the tunnel startup process, in which a ruptured diaphragm generates an expansion fan. Rather, a conventional "impulsive" start is used to arrive at a steady solution. Numerical simulations were performed using GASPex Version 4.1.0[11], with an implicit dual time stepping algorithm and a time step of 10^{-6} sec. Each case was run until unstart occurred or until it appeared steady (10-20 ms).

Table 1: Boundary conditions

	Empty Section	**Section with Cone**
Inflow	pointwise data from EDDYBL	pointwise data from EDDYBL
Outflow	forced outflow	forced outflow
Top	no slip, isothermal 540°R (300 K)	no slip, adiabatic
Centerline	symmetry plane	symmetry plane
Cone Surface	---	no slip, adiabatic

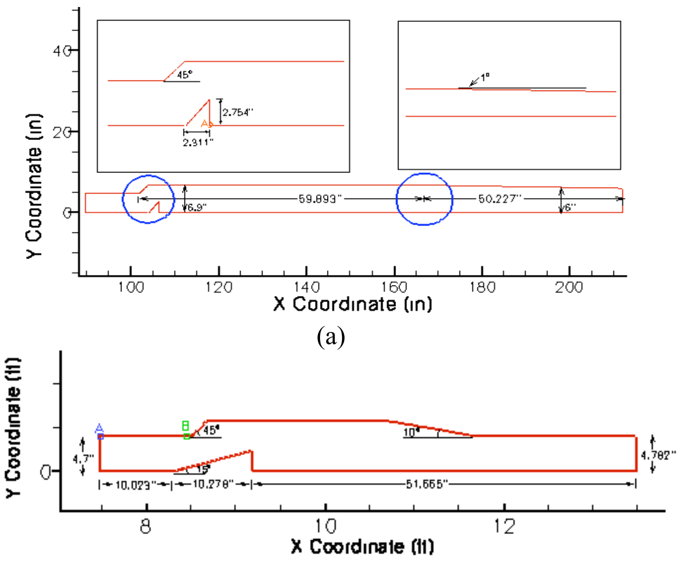

(a)

(b)

Figure 3: Computational domain for 50° (a) and 15° (b) half-angle cones

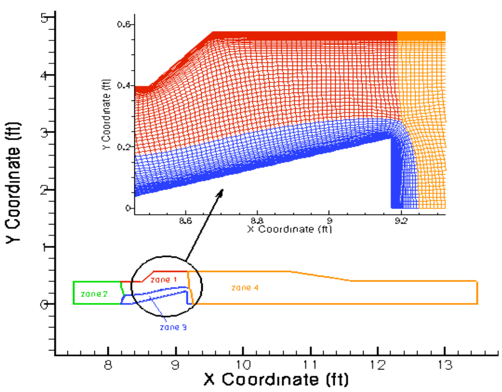

Figure 4: Zone decomposition and grid clustering for 15° case

3. Results

First, the flowfield in the test section is examined with and without the 15° half-angle cone. The angle of the cone is then increased to determine the bluntest cone that will fit in the tunnel without causing unstart.

3.1 Empty section and section with 15° half-angle cone

Figure 5 shows numerical schlieren images of the flowfield in the test section with and without a cone. A shear layer appears at the 45° expansion corner and a series of shocks turn the flow back at the 10° compression corner. A recirculation region exists in the wake of the cone and in the expansion corner (Figure 6).

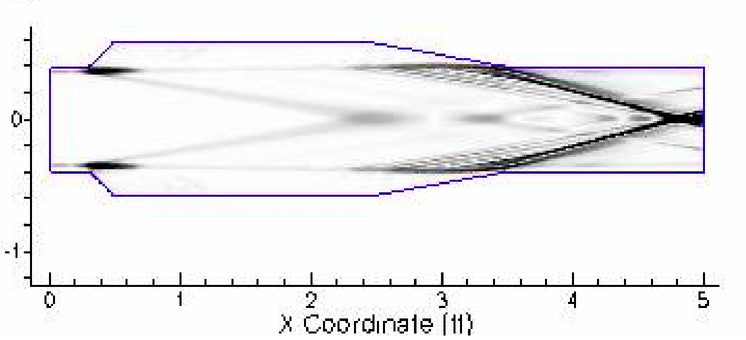

(a)

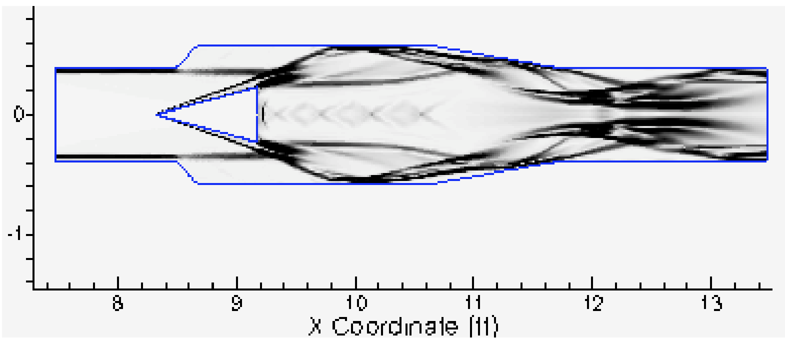

(b)

Figure 5 : Schlieren image at t=20 ms for empty section (a) and 15° half-angle cone (b)

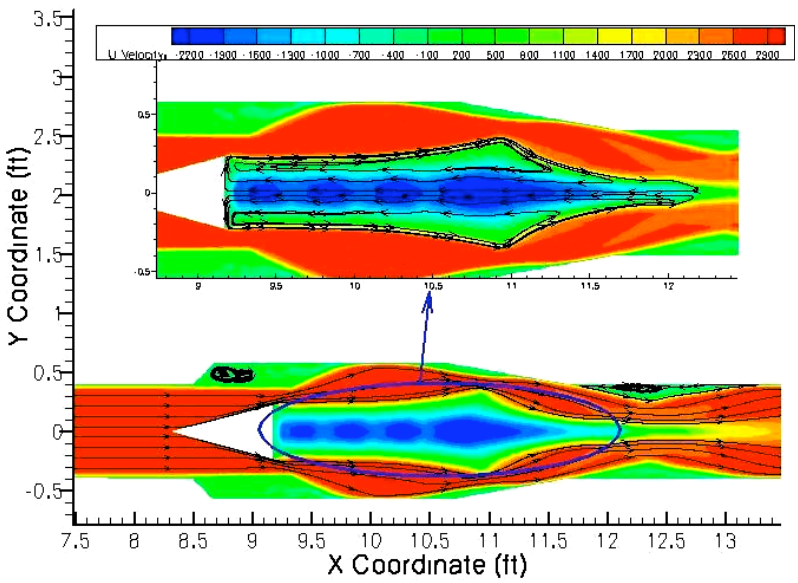

Figure 6 : Streamlines and u-velocity (ft/sec) contours in recirculation regions at t=20 ms for 15° half-angle cone

In order to distinguish between shocks, shear layers and expansion waves, it is helpful to examine various contour plots. Entropy changes across a shear layer but not across an expansion, and there is a noticeable change across a normal shock. Pressure changes across expansion fans and shocks, but not across shear layers. Mach number changes across all three. The structure of the flowfield is illustrated in Figures 7-9 with contour plots superimposed on numerical schlieren images for the 15° half-angle cone at 20 ms.

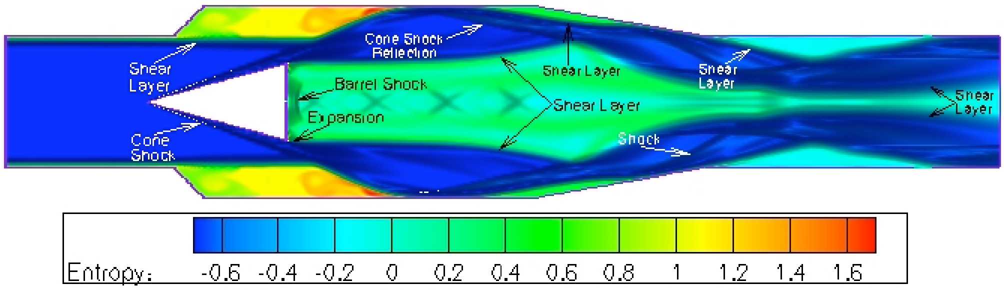

Figure 7: Entropy contours and numerical schlieren for 15° half-angle cone at 20 ms

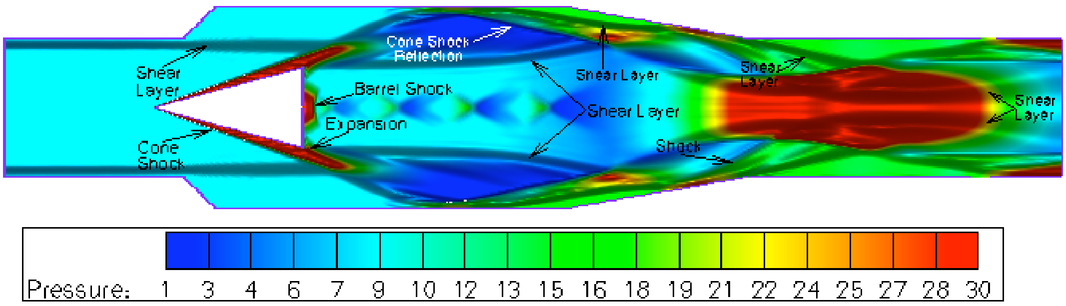

Figure 8: Pressure (lb/ft^2) contours* and numerical schlieren for 15° half-angle cone at 20 ms

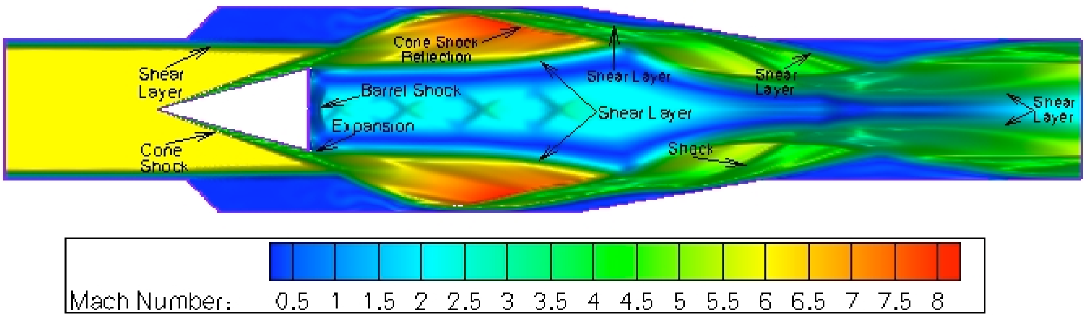

Figure 9: Mach number contours and numerical schlieren for 15° half-angle cone at 20 ms

The flow is unable to make the sharp 45° turn so a shear layer is formed and a recirculation region exists in the extended region. A series of shocks gradually turn the flow at the 10° compression corner so that it exits normal to the outflow boundary. When the flow reaches the cone, a shock forms, which interacts first with the shear layer and then with the boundary layer along the wall. When it hits the wall it reflects off, providing much of the compression needed for the flow to turn the 10° corner. At the base corners of the cone there is a small expansion fan which causes the flow to expand to M ~ 8 (red regions in Figure 9).

A recirculation region exists behind the cone (Figure 6) with a supersonic region in the center (Figure 9). The schlieren image reveals a criss-cross pattern in the wake of the cone (Figure 5) and the pressure contours display a sequence of expansions and compressions (blue and green contours in Figure 8). The flow is moving from right to left, towards the base of the cone, and encounters this series of expansion and compression waves. An expansion

---

* The range of pressures in this plot is limited to pressures below 30 lb/ft^2 for the purpose of distinguishing the pressure variation in the wake of the cone. The pressures in the red area downstream of the compression corner exceed 70 lb/ft^2 and a different choice of contours would illuminate variation in this region as well.

wave accelerates the flow and reflects off the bounding shear layer as a compression wave, which decelerates the flow and increases the pressure. The compression wave then reflects off the shear layer as an expansion wave. This process continues in jet-like fashion, giving rise to the criss-cross pattern. The flow is finally brought to rest by a barrel shock, which slows the flow to stagnation conditions at the cone base.

The region of interest is that upstream of the cone. These computations do not reveal any disturbances to the nozzle-wall boundary layer in this region. All the shock /shear layer/ boundary layer interactions affect the flow downstream of the cone, but do not appear to cause the boundary layer upstream to become unsteady.

3.2 Section with 75° – 30° half-angle cones

The blunter cones appear in Figures 10-12. A separation bubble forms at the expansion corner and bleeds out into the uniform flow. For cones with half-angles from 30° to 75°, the bubble continues to grow until it reaches the inflow boundary, unstarting the tunnel (Figure 13). The u-velocity at the inflow boundary becomes negative, even though the boundary condition is trying to force the flow forward. At this point, the results cease to be meaningful and the computation is stopped.

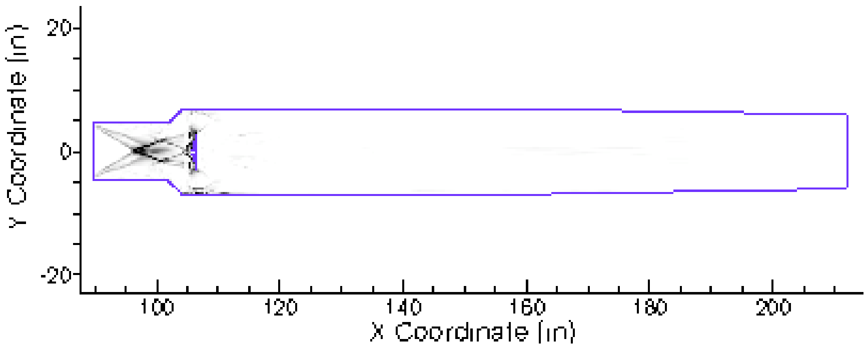

Figure 10: Schlieren snapshot at 4 ms – 75° half-angle cone

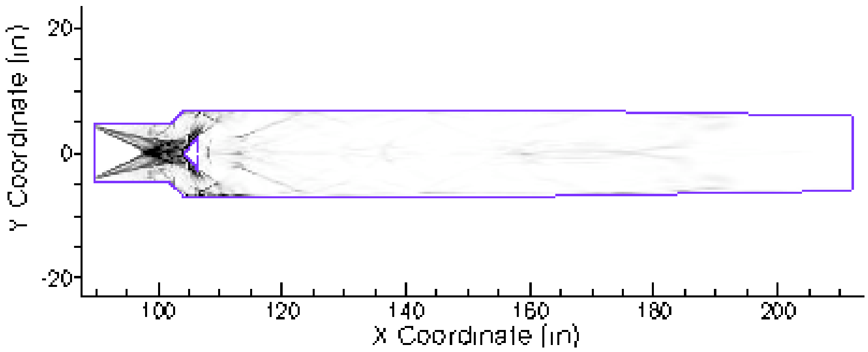

Figure 11: Schlieren snapshot at 4 ms – 50° half-angle cone

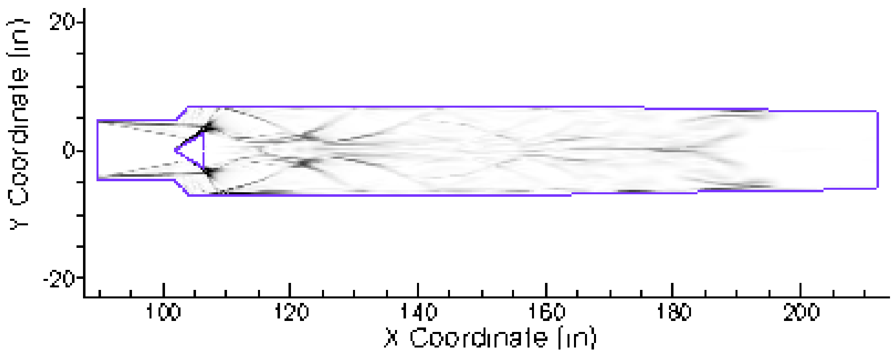

Figure 12: Schlieren snapshot at 4 ms – 30° half-angle cone

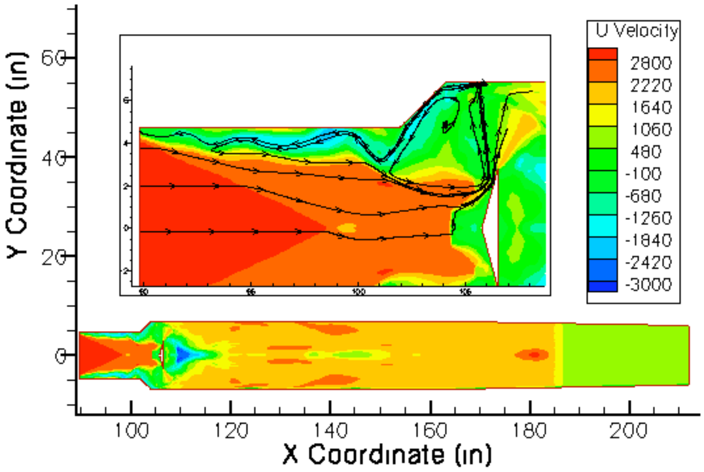

Figure 13: U-velocity contours with streamlines of 75° half-angle cone unstarting the tunnel

3.3 Section with 20° half-angle cone

The 20° half-angle cone is shown in Figure 14. This appears to be a stable configuration. There is a very small upstream influence (Figure 15) where the separation bubble spreads beyond the expansion corner, but unlike with the blunter cones, this separation bubble is steady and it never reaches the upstream boundary.

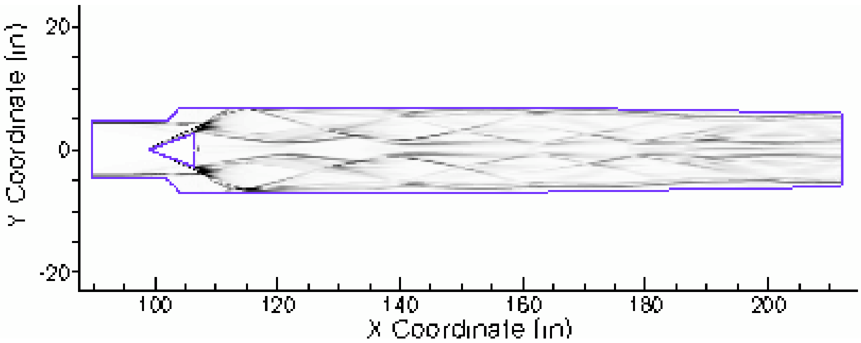

Figure 14: Schlieren image of developed flowfield at 9.5 ms -- 20° half-angle cone

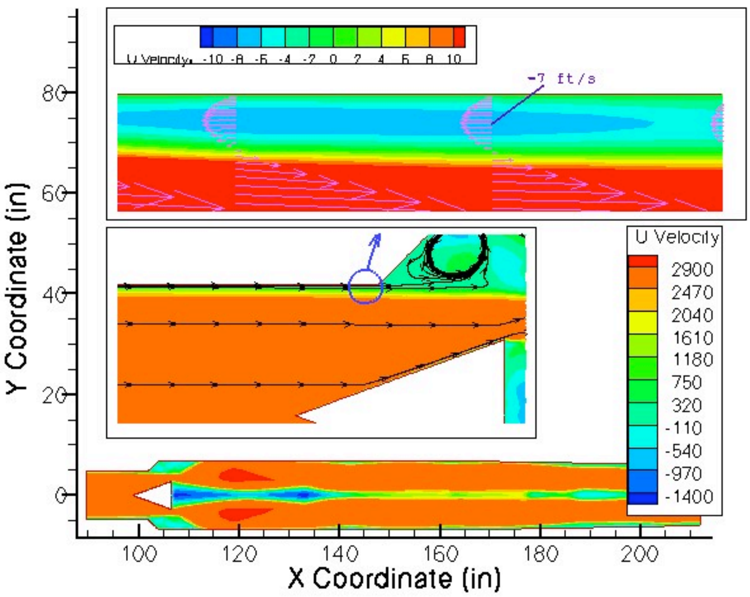

Figure 15: U-velocity contours and streamlines for the 20° half-angle cone

4. Conclusion

CFD is used to evaluate a new design for the test section of the BAM6QT. Bow shocks from the models interact with the nozzle wall boundary layer and can propagate upstream in the boundary layer and induce separation. In this study the diameter of the test section is expanded so that shock waves from the nose of the model interact with a shear layer before hitting the wall boundary layer, in the hopes that this would prevent the upstream propagation of disturbances in the boundary layer. The expansion generates shear layers and expansion waves that interact with each other and with the bow shock from the model. The flowfield in this section is examined to determine if any of these interactions cause disturbances to propagate upstream into the quiet test region.

Several cone sizes, with half-angles ranging from 15° to 75°, are investigated to determine if they would unstart the tunnel. It was found that a 15° half-angle cone fit into the modified section without causing any upsream separation, but the 30°-75° half-angle cones unstart the tunnel. The 20° half-angle cone seems to be stable and the separation bubble that forms in the corner moves only slightly upstream and remains in place. Although the tunnel is not unstarted, the disturbances due to this small, upstream separation bubble may generate noise that interferes with laminar measurements. This upstream effect is not evident in the 15° half-angle case, which is an improvement over the 7° half-angle cone currently used. These are preliminary computations for the expanded test section, which is to be installed over the summer. Investigation into this issue will continue during the fall as the new section is tested.

References

[1] Beckwith, I. E., Chen, F. J. and Creel, T. R. Design requirements for the NASA Langley supersonic low disturbance wind tunnel. *14th Aerodynamic Testing Conference*, AIAA-1986-763, March 1986.
[2] Reed, H., Kimmel, R., Schneider, S. and Arnal, D. Drag prediction and transition in hypersonic flow. *28th AIAA Fluid Dynamics Conference*, AIAA-1997-1818, June-July 1997.
[3] Schneider, S. P. The development of hypersonic quiet tunnels. *37th AIAA Fluid Dynamics Conference*, AIAA-2007-4486, June 2007.
[4] Schneider, S. P., Juliano, T. J. and Borg, M. P. High-reynolds-number laminar flow in the mach-6 quiet-flow ludwieg tube. *36th AIAA Fluid Dynamics Conference*, AIAA-2006-3056, June 2006.
[5] Schneider, S. P. Laminar-turbulent transition on reentry capsules and planetary probes. *Journal of Scpacecraft and Rockets*, 43:1153-1173, 2006.
[6] Skoch, C., Schneider, S. P. and Borg, M. P. Disturbances from shock/boundary-layer interactions affecting upstream hypersonic flow. *35th Fluid Dynamics Conference*, AIAA-2005-4897, June 2005.
[7] Pope, A. and Goin, K. High-speed wind tunnel testing. Wiley, New York, 1965.
[8] Skoch, C. R. Disturbances from shock/boundary-layer interactions affecting upstream hypersonic flow. PhD thesis. Purdue University School of Aeronautics and Astronautics, December 2005.
[9] Program Development Corporation. *GridPro/az3000 User's Guide and Reference Manual*.
[10] Wilcox, D. C. Turbulence modeling for CFD (3rd ed.). DCW Industries, California, 2006.
[11] Aerosoft Inc. *General Aerodynamic Simulation Program User Manual*.

This page has been purposedly left blank